Carboxy-Terminal Extension Effects on Crystal Formation and Insecticidal Properties of Colorado Potato Beetle-Active *Bacillus thuringiensis* δ-Endotoxins

Samir Naimov,[1] Elena Martens-Uzunova,[1] Mieke Weemen-Hendriks,[2] Stefan Dukiandjiev,[1] Ivan Minkov,[1] and Ruud A. de Maagd[2,]*

Abstract

Many *Bacillus thuringiensis* crystal proteins, particularly those active against lepidopteran insects, have carboxy-terminal extensions that mediate bipyramidal crystal formation. These crystals are only soluble at high (>10.0) pH in reducing conditions such as generally found in the lepidopteran midgut. Most of the Colorado potato beetle (CPB)-active toxins lack such an extension, yet some toxins with a carboxy-terminal extension have cryptic activity against this insect, revealed only after in vitro solubilization. Crystal formation, morphology, protein content, and activity against CPB were compared for two sets of proteins, the Cry1-hybrid SN19 and Cry3Aa, both with and without a carboxy-terminal extension. Cry3Aa, with or without extension, formed flat square or rectangular crystals. SN19 (with extension) and its derivative without extension formed irregular inclusion bodies. All Cry3Aa and SN19 crystals and inclusion bodies were almost equally active before and after in vitro presolubilization and could be solubilized in diluted CPB midgut extract. In contrast, bipyramidal crystals of Cry1Ba were insoluble under these conditions. Our results suggest that bipyramidal crystal formation typical for proteins with a carboxy-terminal extension may preclude activity against CPB, but that interfering with this crystal formation can increase the activity.

Index Entries: *Bacillus thuringiensis*; Colorado potato beetle; crystal protein; disulfur bridges.

1. Introduction

Bacillus thuringiensis and some related Gram-positive, sporulating bacterial species produce a large variety of proteins with insecticidal properties, often deposited as crystals during sporulation ***(1)***. Possible purposes suggested for the occurrence of such crystals are protection against fast solubilization and degradation in the environment, protection against extracellular proteases produced by the mother cell, and more recently, protection against toxicity of the amino-terminal part of the protoxin to *B. thuringiensis* itself ***(2)***.

Most Cry1 proteins from *B. thuringiensis*, which are in general active against Lepidoptera, have a carboxy-terminal extension that is required for their bipyramidal crystal formation. This carboxy-terminal extension, as opposed to the amino-terminal part, is rich in cysteins, which form intermolecular sulfur bridges in the crystal lattice, explaining the solubility of these crystals at the high pH typical for lepidopteran and dipteran larvae, in the presence of reducing agents ***(3)***. After ingestion by the insect, the crystal is solubilized and the protoxin is processed by proteases to an active form of approx 65 kDa. In this

*Author to whom all correspondence and reprint requests should be addressed.[1]Department of Plant Physiology and Molecular Biology, University of Plovdiv, Plovdiv, Bulgaria. [2]Business Unit Bioscience, Plant Research International B.V, P.O. Box 16, 6700 AA Wageningen, The Netherlands. E-mail: Ruud.deMaagd@wur.nl.

Molecular Biotechnology © 2006 Humana Press Inc. All rights of any nature whatsoever reserved. 1073–6085/2006/32:3/185–196/$30.00/Online ISSN: 1559-0305

process, the carboxy-terminal half (500–600 amino acids), as well as around 30 amino acids at the amino-terminus are removed, and thus play no direct role in the toxic action of the protein. The activated toxins consist of three structural domains with distinct functions in receptor binding and pore formation (for review, *see* **ref. *1***). The efficiencies of solubilization of crystals and of proteolytic activation of protoxins play a role in determining activity ***(4,5)***. Insect midgut proteases as well as midgut pH, and possibly DNases, play an essential role in that process ***(6,7)***.

The coleopteran-specific Cry3Aa crystal protein shares amino acid sequence similarity and the three-domain structure with the processed lepidopteran-specific Cry1 toxins, but is not synthesized and stored as a large protoxin. The 73-kDa Cry3A protein forms a flat rectangular crystal inclusion in *B. thuringiensis* ***(8)***. The crystal is probably packed by ionic interactions and can be solubilized at neutral pH without reducing agents, matching well the conditions in many Coleoptera, including the important potato pest, Colorado potato beetle (CPB; *Leptinotarsa decemlineata*-Say), for which Cry3Aa is the single most active protein ***(9)***.

Despite the fact that Cry1 proteins are generally active against Lepidoptera, two proteins, Cry1Ba and Cry1Ia, have been shown also to have some activity against coleopterans. Among those insects is CPB, although the toxicity of Cry1Ba and Cry1Ia for CPB was much lower than that of Cry3Aa ***(10,11)***. However, Cry1Ba crystals were active only after in vitro presolubilization at pH 10.0 ***(11)***, suggesting that the presence of a carboxy-terminal extension and the resulting formation of bipyramidal crystals may preclude solubilization in the coleopteran midgut, which generally has a pH of 6.0–7.0 ***(12)***. Furthermore, Cry7A, which also contains a carboxy-terminal extension and forms bipyramidal crystals, was active against CPB only after in vitro presolubilization at high pH followed by in vitro activation by trypsin or CPB gut secretions ***(13)***.

During our previous research, a Cry1 hybrid protein consisting of Cry1Ba with its domain II replaced by that of Cry1Ia (SN19) and with increased activity against CPB was created ***(14)***. Expression of a truncated SN19 gene in transgenic potato plants led to resistance to CPB, as well as to the lepidopteran pests European corn borer (*Ostrinia nubilalis*) and potato tuber moth (*Phthorimaea operculella*) ***(15)***. The previous observations with Cry1Ba and Cry7Aa suggested that the presence of a carboxy-terminal extension in SN19, absent in previously described highly CPB-active δ-endotoxins, might limit the usefulness of SN19 in spore/crystal preparations for CPB control as an alternative for transgenic plants.

To investigate the effect of the carboxy-terminal extension, two sets of proteins were produced in *Escherichia coli* and in an acrystalliferous strain of *B. thuringiensis*. By in vivo recombination, we obtained a hybrid gene encoding Cry3Aa with the carboxy-terminal extension of Cry1Ba. Through a systematic analysis of SN19 and Cry3Aa versions, with or without the Cry1Ba carboxy-terminal extension, we were able to investigate the role of the extension (and of its interaction with the active toxin-encoding part) in crystal formation and in activity against CPB.

2. Materials and Methods

2.1. Expression Vectors for Escherichia coli

All Cry protein expression vectors and "tandem" plasmids are based on pBD10, a derivative of pKK233-2 ***(16)***. Cry1Ba, SN19, and Cry3Aa expression vectors pMH19, pSN19, and pMH10, respectively, have been described earlier ***(14,17)***.

For the construction of a truncated version of SN19, the domain III encoding part of *SN19* was amplified using the following primer pair: (forward) BIB12.1fosf (5'-GAACAAGTTACCATCTACAG CTTGTTGAGTCGTGGA) and (reverse) BIBtrR: (5'-GGCGGATCCTAAACTGG AATAA TTTCAATTTTATC) (Eurogentec, Seraing, Belgium). Through this polymerase chain reaction (PCR) reaction, a stop-codon and *Bam*HI restriction site were introduced at position 1918 and 1923, respectively. The PCR product was digested with *Mun*I and *Bam*HI, run on a 0.8% agarose gel, excised and purified using a QIAEX II agarose gel extraction kit (Qiagen, Oslo, Norway), and

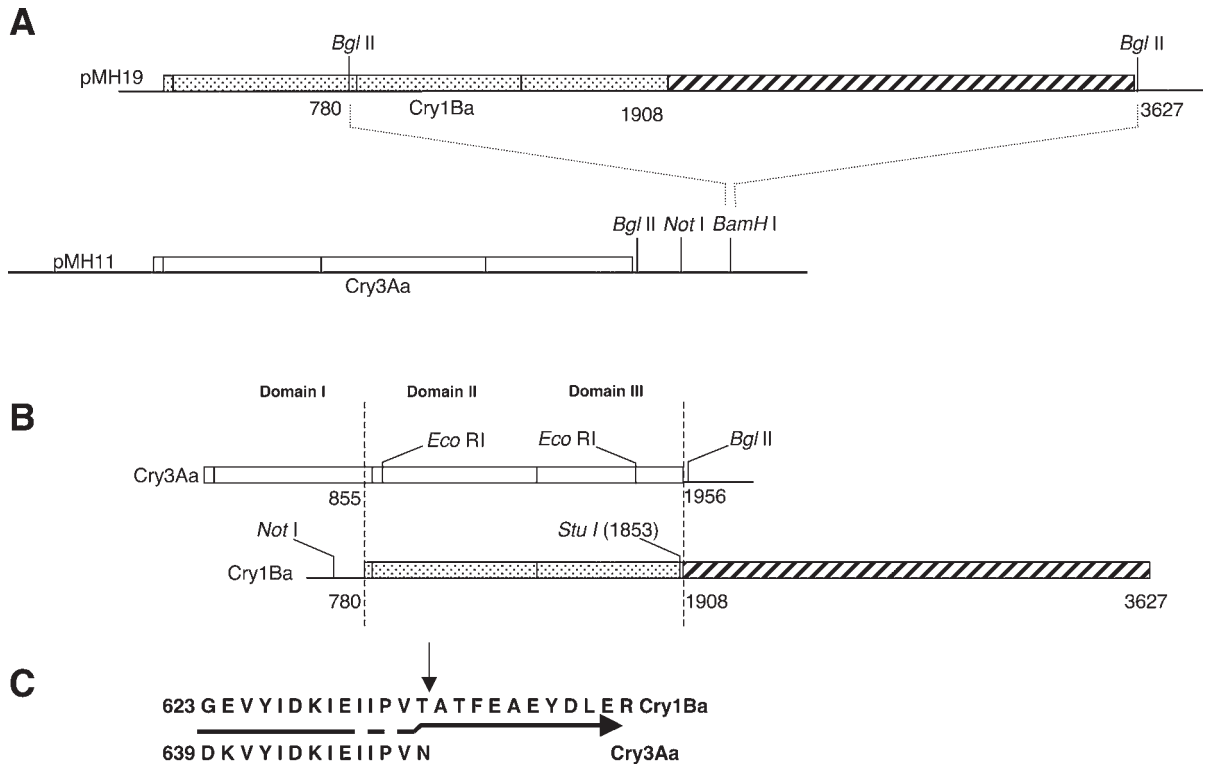

Fig. 1. Tandem plasmid for in vivo recombination of *cry3Aa* and *cry1Ba*. **(A)** Construction of tandem plasmid pSN5. A *Bgl*II fragment of *cry1Ba* from plasmid pMH19 was inserted into the *Bam*HI site of plasmid pMH11 (containing *cry3Aa*), resulting in the two genes cloned in tandem. The three domains of the activated toxin are indicated by dotted shading for Cry1Ba. The short amino-terminal and longer carboxy-terminal extension (for Cry1Ba) are indicated by hatched shading. **(B)** Schematic representation of the insert of plasmid pSN5. The overlapping homologous parts of Cry3Aa and Cry1Ba are vertically aligned, whereas in reality they are placed in tandem. The *Not*I and *Bgl*II, restriction sites of the intervening polylinker, used for selecting recombinants are indicated, as are the sites used for localization of recombination events. **(C)** Detail of an amino acid alignment of Cry3Aa and Cry1Ba indicating the area of cross-over in EU3. The arrow indicates where for production of SN19tr, a stop codon, was inserted (*see* **Fig. 2A**).

subsequently used to replace the *Mun*I–*Bam*HI fragment of pSN19 encompassing the domain III and carboxy-terminal extension coding region of the *SN19* gene (*see* diagram in **Fig. 2A**). This resulted in truncated SN19 (SN19tr) expression vector pSN50.

2.2. Cry3Aa/Cry1Ba Hybrids

A *Bgl*II fragment from pMH19 containing bases 780–3527 of *cry1Ba* was cloned into the *Bam*HI site of the polylinker of pMH11, resulting in *cry3Aa*/*cry1Ba* tandem plasmid pSN5 (**Fig. 1A, B**). Following the earlier described strategy for in vivo recombination of tandem plasmids ***(16)***, pSN5 was extracted from *E. coli* strain JM101, digested with *Not*I and *Bgl*II to select for recombination events, and then used to transform *E. coli* strain XL1-blue (**Fig. 1B**). Plasmid DNA was extracted from the resulting transformants, subjected to restriction enzyme analysis and finally DNA sequencing to identify true recombinants and to locate the cross-over site.

2.3. Protein Isolation From E. coli XL-1 Blue and Insect Bioassays

For fast screening of soluble protoxin formation in recombinant clones, a previously described procedure was used ***(18)***. The resulting pellets of

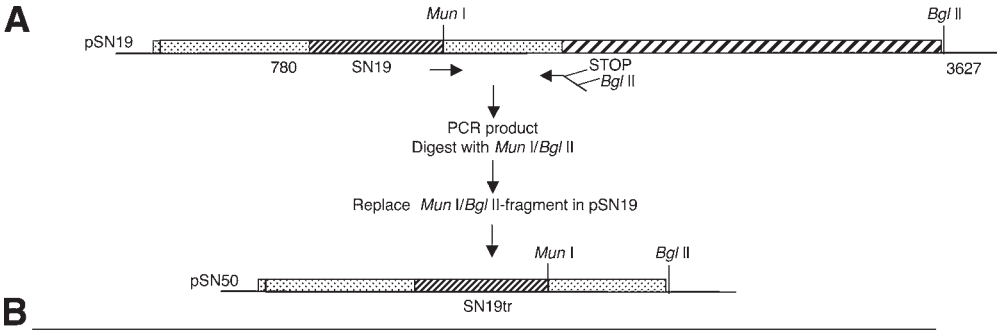

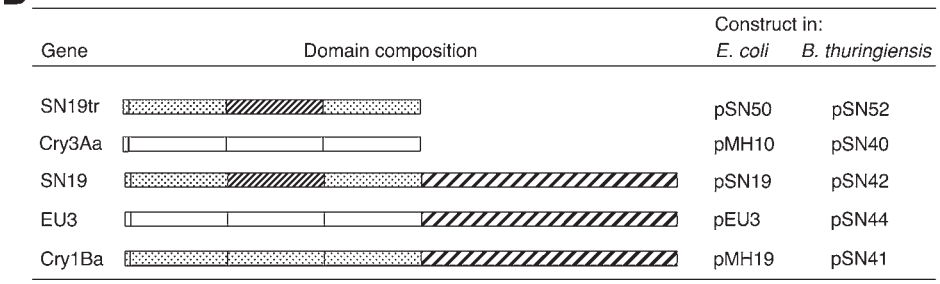

Fig. 2. Construction of the gene encoding SN19tr and plasmids used in this study. **(A)** Strategy for the truncation of the SN19 gene resulting in plasmid pSN50. **(B)** Domain composition and plasmid names of the proteins used in this study. The shading of the three structural domains of activated toxin encoding parts indicates their origin. No shading: Cry3Aa; dotted shading: Cry1Ba; fine hatched shading: Cry1Ia.

inclusion bodies were incubated in solubilization buffer (50 m*M* $NaHCO_3$, 100 m*M* NaCl, 10 m*M* DTT, pH 10.0) and screened for the presence of soluble protoxin by sodium dodecyl sulfate (SDS)-polyacrylamide gel electrophoresis (PAGE) of the supernatant. For large-scale production, all parental and hybrid protoxins were expressed in *E. coli* strain XL-1 Blue and extracted as described earlier ***(19)***. Solubilized protoxins were dialyzed overnight against 25 m*M* $NaHCO_3$, 100 m*M* NaCl, pH 10.0. Protein concentrations were estimated by scanning of Coomassie-stained SDS-polyacrylamide gels containing toxin preparations and comparison to a bovine serum albumin calibration curve (0–750 ng) using the Gel-Pro Analyzer 3.1 software package (Media Cybernetics, Silver Spring, MD). To test toxicity for CPB, leaflets of greenhouse-grown potato cultivar Desiree were dipped in toxin dilutions in water containing 0.01% Tween-20. After air-drying the leaves, they were transferred to Petri dishes and 10 neonate CPB larvae were placed on each leaf. After incubation for 2 d at 28°C, the leaves were replaced by fresh leaves dipped in freshly prepared protoxin dilutions. Mortality was scored after 4 d. LC_{50} (concentration with 50% mortality) and 95% fiducial limits were estimated by Probit analysis of results from three or more independent experiments, using the PoloPC computer program ***(20)***.

2.4. Shuttle Vectors and B. thuringiensis *Transformation*

The vector pSB629, a derivative of pBluescriptKS$^+$ containing the *cry1Ca* gene between its own promoter and the *cry1Ac* terminator, and the shuttle vector pSB634, a derivative of pBluescriptKS$^+$ and pBC16-1, have been described before ***(18,21)*** and were kindly provided by T. Yamamoto.

To clone *cry3Aa* gene between the *cry1Ca* promoter and *cry1Ac* terminator, the *Nco*I–*Sma*I (*cry1Ca*) fragment of pSB629 was replaced by the *Nco*I–*Sma*I (*cry3Aa*) fragment of pMH10. The resulting plasmid (pSN35) was digested with *Apa*I–*Sst*I, and the whole expression cassette was

cloned into the *Apa*I–*Sst*I sites of pSB634 giving pSN40. The *SN19* gene was cloned in the expression cassette by replacing the *Nco*I–*Bam*HI (*cry1Ca*) fragment of pSB629 by that of pSN19, resulting in pSN37, followed by *Apa*I–*Pst*I subcloning of the expression cassette in pSB634, resulting in pSN42. The *cry1Ba*, *EU3* hybrid, and truncated *SN19* genes were cloned in pSB629 by substitution of the *Nco*I–*Bgl*II fragment of *cry1Ca* in pSB629, giving pSN36, pSN39, and pSN51, respectively. *Cry1Ba*- and *EU3*-harboring expression cassettes were subcloned in the *Apa*I–*Pst*I sites of pSB634, resulting in pSN41 and pSN44. The shuttle vector containing the truncated *SN19* gene-expression cassette (pSN52) was obtained by *Apa*I–*Sst*I subcloning in pSB634.

Shuttle vectors were introduced via *E.coli* strain GM2163 (*dam*, *dcm*, *hsdR*) into the *cry*-negative *B. thuringiensis* strain Bt51 by electroporation, as described previously ***(18)***. Aliquots were plated on Luria broth (LB) plates containing 20 μg/mL tetracycline as a selective antibiotic and grown overnight at 28°C.

2.5. Bacillus thuringiensis *Crystal Preparation and Insect Bioassays*

Flasks of 1 L containing 200-mL CYS sporulation medium ***(22)*** were inoculated with a single colony and incubated in a rotary shaker at 28°C and 280 rpm. Progress of sporulation was monitored by phase-contrast light microscopy. When 75–80% of the cells had reached sporulation (producing free spores), cultures were harvested, treated overnight with 0.1 mg/mL lysozyme at 30°C, washed five times with TEN buffer (20 m*M* Tris-HCl, pH 8.0, 2 m*M* EDTA, and 1 *M* NaCl) and twice with demineralized water. Subsequently, the crystals were purified in a discontinuous sucrose gradient as described before ***(23)***. The amount of the crystal protein was estimated by SDS-PAGE. The protease inhibitor cocktail CompleteR (Roche Diagnostics GmbH, Mannheim, Germany) was added before electrophoresis, according to the manufacturer's instructions.

To test toxicity of the crystal suspensions and solubilized proteins for CPB, leaf-dip bioassays were performed as described previously, except that Tween-20 was substituted by 0.01% Tween-80. For the purpose of comparison of toxicity of crystal spore preparations with toxicity of presolubilized crystals, a dose equal to the previously determined LC_{50} was used (1.8 μg/mL for Cry3Aa, 1.6 μg/mL for EU3 [this study], and 7.9 μg/mL for SN19 ***[14]*** and SN19tr). The crystal preparations were solubilized in carbonate buffer (25 m*M* $NaHCO_3$, 100 m*M* NaCl, and 10 m*M* DTT, pH 10.0) for 2 h at 37°C. The completeness of solubilization was checked by SDS-PAGE. The averages of percentages of mortality and their standard deviations were determined from results of three independent experiments.

2.6. Colorado Potato Beetle Midgut Extract Treatment of Crystals

CPB midgut tissue (25 mg) was ground in a microcentrifuge tube and suspended in 100 μL of sterile distillated water. After centrifugation at 15,000*g* for 30 min at 4°C in an Eppendorf 5417R centrifuge, the protein concentration of the supernatant was determined. Midgut extract was added to each crystal preparation at a 10% (w/w) extract protein/crystal protein–ratio, and samples were incubated at room temperature for times varying from 10 min to 2 h. For each time point, 1 μg of crystal protein was used. The final pH of the reaction mixture was 6.5–7.0. To prevent further proteolytic processing of samples, 1 m*M* PMSF and 5 m*M* EDTA were added at the end of the incubation period. Nonsolubilized crystals were pelleted by centrifugation at 15,000*g* for 10 min at 4°C. Aliquots from the supernatant, containing solubilized crystal proteins were analyzed on 10% SDS-polyacrylamide gels.

2.7. Scanning Electron Microscopy

Scanning electron microscopy investigations were performed in the Central Laboratory of Geology and Mineralogy, Bulgarian Academy of Science, Sofia. The crystal spore preparations of transformed *B. thuringiensis* strain Bt51 were air-dried and coated with gold for 5 min. Mounts were examined and photographed in a Philips SEM454 electron microscope at a voltage of 20 kV.

3. Results

3.1. cry3Aa/cry1Ba Hybrids

To study the properties of Cry3Aa/Cry1Ba hybrid proteins, we set out to construct a *cry3Aa/cry1Ba* hybrid library using the in vivo recombination strategy ***(16,18)***. Overlapping parts of the parental genes *cry3Aa* and *cry1Ba* (in that order), with part of the pBluescript SK^+ linker in between were cloned in tandem in the plasmid pSN5 (**Fig. 1A**), and introduced in the strain *E. coli* JM101 (*RecA*$^+$). The DNA, extracted from *E. coli* JM101, was digested with *Not*I and *Bgl*II (**Fig. 1B**), and retransformed to *E. coli* strain XL-I Blue for selection of recombinants. Restriction analysis of plasmids from transformants showed that approx 50% of the plasmids contained inserts of the size (approx 3550 bp) expected for proper recombinants. In total, 46 recombinants were subjected to restriction analyses for localization of cross-over sites. There appeared to be a very strong bias (30 recombinants) for cross-overs downstream (3') of the *Stu*I site (position 1853) of *cry1Ba* (*see* **Fig. 1B**), corresponding to the region encoding the very carboxy-terminal part of domain III. Of the 10 recombinants from this group that were tested for production of a soluble protoxin, all proved to be positive. Sequencing of two of those revealed an identical cross-over site in the very 3' part of *cry3Aa*, producing a hybrid gene consisting of the full *cry3Aa* protoxin encoding part with the *cry1Ba* protoxin-specific carboxy-terminal encoding fragment (**Fig. 1C**). Only one of those, EU3, was used for further study. Of the other recombinants, two cross-overs were located in front of the *Eco*RI sites of *cry3Aa*, whereas 14 were located in between those *Eco*RI sites (**Fig. 1B**). None of those recombinant genes expressed soluble protoxins in *E. coli*.

On analysis by SDS-PAGE, solubilized Cry3Aa protein appeared as a major band with molecular weight of approx 75 kDa together with an often-seen minor band, which may be, as has been reported earlier ***(24,25)***, the product of in vivo (in *B. thuringiensis*) or in vitro proteolysis (**Fig. 3A**, lane 1). Solubilized EU3 protein isolated from *E. coli* appeared mostly as a band with an apparent molecular weight of approx 130 kDa (**Fig. 3A**, lane 2), similar to solubilized SN19 (**Fig. 3A**, lane 3). Toxicity of solubilized Cry3Aa and EU3 protein for CPB were compared in a potato leaf dip assay. The LC_{50} values for Cry3Aa (1.8 μg/mL, 95% fiducity limits: 1.4–2.5) and EU3 (1.6 μg/mL, fiducity limits: 1.2–2.0) were very similar. Thus the hybrid EU3 was fully active against CPB and the presence of a Cry1-derived carboxy-terminal extension did not negatively affect toxicity in a presolubilized state.

3.2. Effects of a Carboxy-Terminal Extension on Crystal Formation, Morphology, and Protein Profiles in B. thuringiensis

To study the role of the Cry1-type carboxy-terminal extension in crystal formation and its effect on activity against CPB, we produced Cry3Aa, the Cry3Aa/Cry1Ba hybrid EU3, the CPB-active Cry1 hybrid SN19, and its truncated form SN19tr in *B. thuringiensis*. The truncated version of SN19 was designed to have a carboxyl terminus similar to that of Cry3Aa (indicated by arrow in **Fig. 1C**), thus completely lacking the carboxy-terminal extension of SN19 and creating two similar-sized versions of each of two CPB-active proteins (**Fig. 2B**). Expressed in *E. coli*, SN19tr formed inclusion bodies, which could be solubilized at pH 10.0 like most Cry1 proteins, and on SDS-PAGE, giving a triplet of bands of approximately the expected apparent molecular weight (**Fig. 3A**, lane 4). Thus, it is likely that the major lower band is the product of limited in vivo or in vitro proteolysis. All four genes were cloned in a shuttle vector and used to transform a *cry*-negative strain of *B. thuringiensis* to observe crystal formation during sporulation.

All four transformants of *B. thuringiensis* strain Bt51 sporulated, and during sporulation formed inclusions, crystalline or otherwise. For comparison of their morphology, crystals were photographed during sporulation using a phase-contrast microscope (**Fig. 4A–D**), and washed spore/crystal preparations were studied by scanning electron microscopy (Fig. **4E–H**). As documented previously, expression of the naturally truncated *cry3Aa* gene resulted in the formation of flat square or rectangular crystals (**Fig. 4A**,**E**). Interestingly, the

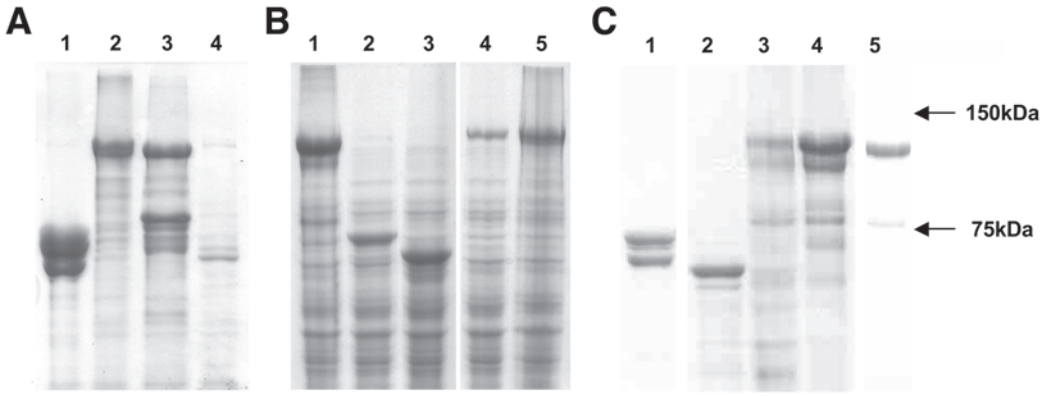

Fig. 3. The SDS-PAGE profiles of proteins isolated from *E. coli* or *B. thuringiensis*. Partially purified inclusion bodies or crystals were solubilized directly in SDS-PAGE sample buffer. **(A)** Expressed in *E. coli* strain XLI-Blue. Lane 1: Cry3Aa (pMH10); lane 2: EU3 (pEU3); lane 3: SN19 (pSN19); lane 4: SN19tr (pSN50). **(B)** Expressed in *B. thuringiensis* strain Bt51. Spore/crystal-mixtures. Lane 1: Cry1Ba (pSN41); lane 2: Cry3Aa (pSN40); lane 3: SN19tr (pSN52); lane 4: EU3 (pSN44); lane 5: SN19 (pSN42). (**C**) Expressed in *B. thuringiensis* strain Bt51. Sucrose gradient-purified crystals. Lane 1: Cry3Aa (pSN40); lane 2: SN19tr (pSN52); lane 3: SN19 (pSN42); lane 4: Cry1Ba (pSN41); lane 5: EU3 (pSN44).

hybrid *EU3* gene encoding Cry3Aa with the carbox-terminal extension of Cry1Ba gave large, regular-shaped, flat, rhomboid, or trapezoid crystals (**Fig. 4B**,**F**).

Both the full-length SN19 and the truncated SN19tr proteins formed multiple smaller, irregular-shaped, or spherical inclusion bodies per sporulating cell. These formed more dense aggregates in cells expressing the full-length gene (**Fig. 4C**) and more distinct inclusions in cells expressing the truncated SN19tr (**Fig. 4D**), but both types of inclusions appeared similar in the scanning electron microscope (**Fig. 4G**,**H**, respectively). These inclusions are clearly different from the regular Cry1-type bipyramidal crystals formed by Cry1Ba (not shown).

Both washed spore/crystal mixtures as well as sucrose gradient-purified crystals were analyzed by SDS-PAGE (**Fig. 3B**,**C**, respectively). Although, in some cases, we observed signs of proteolytic activity associated with the preparations prematurely processing the proteins (more so in purified crystal preparations), all the proteins did appear as bands of approximately the expected molecular weight. Proteins produced in *B. thuringiensis* (**Fig. 3B**) had a similar size as those produced by *E. coli* (**Fig. 3A**), with Cry3Aa showing more of the 75-kDa size compared to *E. coli* (**Fig. 3B**, lane 3). Purified crystal (**Fig. 3C**) showed more or less the same protein profile minus the relatively minor spore proteins, albeit with some signs of further advanced proteolysis, as can be seen by the relatively higher proportion of Cry3Aa appearing as the lower band (**Fig. 3C**, lane 1), and a slight increase in the apparent mobility of SN19tr (**Fig. 3C**, lane 2).

3.3. Effect of a Carboxy-Terminal Extension on Crystal Toxicity Toward Colorado Potato Beetle

Our results show that the addition of a carboxy-terminal extension to Cry3Aa, as in EU3, does not negatively affect activity against CPB when tested as solubilized protein. Results from previous studies on Cry1Ba ***(11)*** and Cry7Aa ***(13)*** hinted that solubilization might be required for EU3 and for SN19 to have activity against CPB when the protein is produced as crystals or inclusions in *B. thuringiensis*. To answer this question, we pair-wise compared Cry3Aa with EU3 and SN19 with SN19tr in bioassays on CPB with intact crystals (or inclusions) as well as with presolubilized proteins. All proteins were tested three times in a single dose, for Cry3Aa and EU3

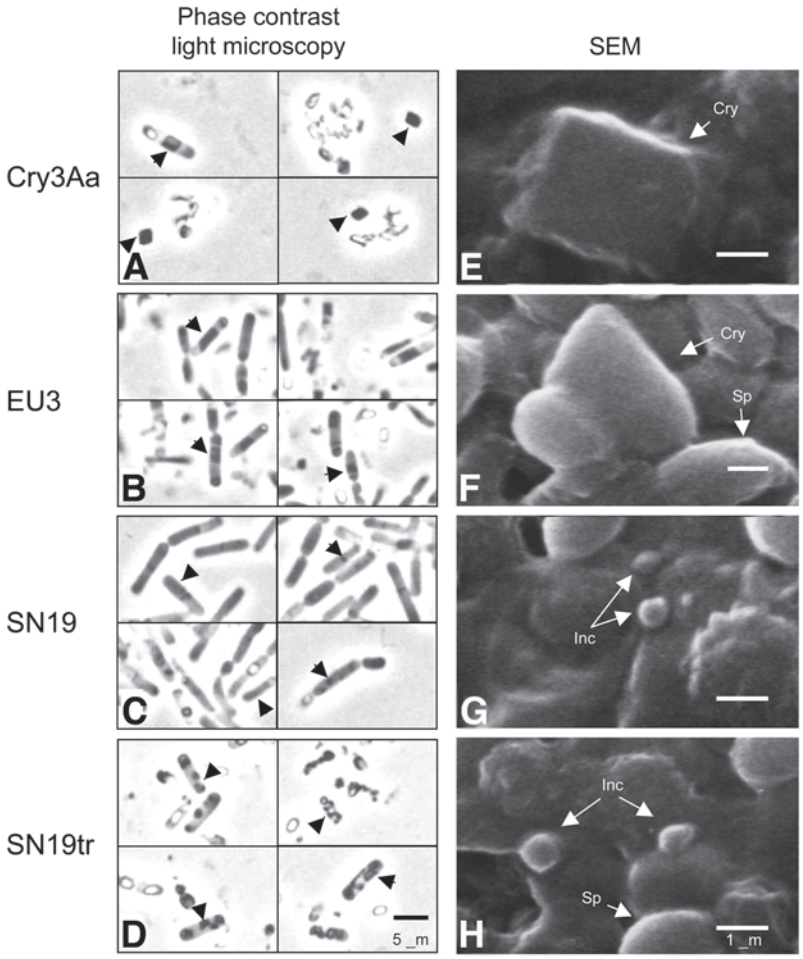

Fig. 4. Morphology of CPB-active delta-endotoxin inclusions produced in recombinant *B. thuringiensis*. **(A–D)** Phase-contrast microscopy. Horizontal bar indicates 5 mm. **(E–H)** Scanning electron microscopy. Arrows indicate crystals and inclusions. Horizontal bar indicates 1 mm. Sp: spore; Inc: inclusion bodies; Cry: crystal.

equal to the dose expected to give approx 50% mortality (1.8 μg/mL or 25 pmol/mL for Cry3Aa, 1.6 μg/mL or 11 pmol/mL for EU3), and for SN19 and SN19tr equal to the dose of SN19 expected to give 50% mortality (7.9 μg/mL, 59 and 100 pmol/mL, respectively). Results of the comparisons are shown in **Fig. 5**. When pair-wise comparing nonsolubilized crystals or inclusion bodies, it appeared that EU3 was as toxic as Cry3Aa, and that SN19 was as toxic as SN19tr. Thus, the presence of the carboxy-terminal extension on either Cry3Aa (as in EU3) or on SN19tr (as in SN19 itself) did not negatively affect activity of these crystals or inclusion bodies against CPB. Moreover, when activity before and after solubilization of crystals was compared for each toxin, the extended versions EU3 and SN19 did not behave differently from their truncated counterparts. For both EU3 as well as Cry3Aa, activity increased significantly after solubilization (Student's *t*-test, $p < 0.05$), whereas for both SN19 as well as SNtr, it slightly decreased, although not as significantly ($p = 0.08$).

3.4. CPB-Active Crystals or Inclusion Bodies Are Effectively Solubilized and Activated by CPB Gut Juice

The apparent lack of effect of in vitro solubilization on the activity of inclusions or crystals of

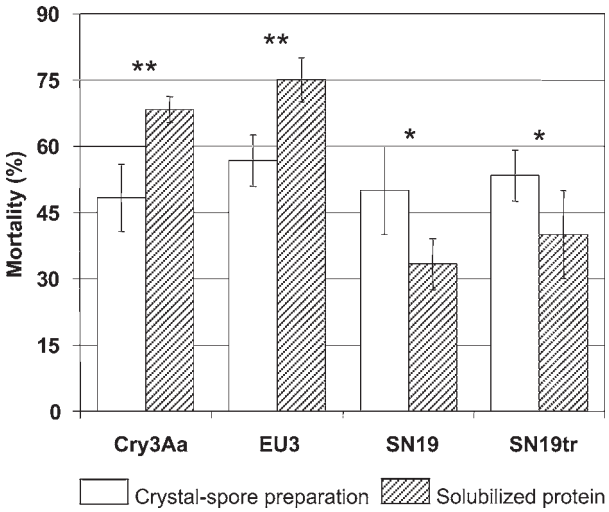

Fig. 5. Comparison of CPB mortality between crystals and presolubilized crystals. Bioassays were performed on neonate CPB in potato leaf dip assays with a single dose of each toxin, either without (open bars) or with presolubilization of the crystals (hatched bars). Mortalities are averages of three experiments. Standard deviations are indicated. **: For both EU3 as well as Cry3Aa activity increased significantly after solubilization (Student's *t*-test, $p < 0.05$), whereas for SN19 as well as SN19tr it slightly decreased, although not as significantly (* $p = 0.08$).

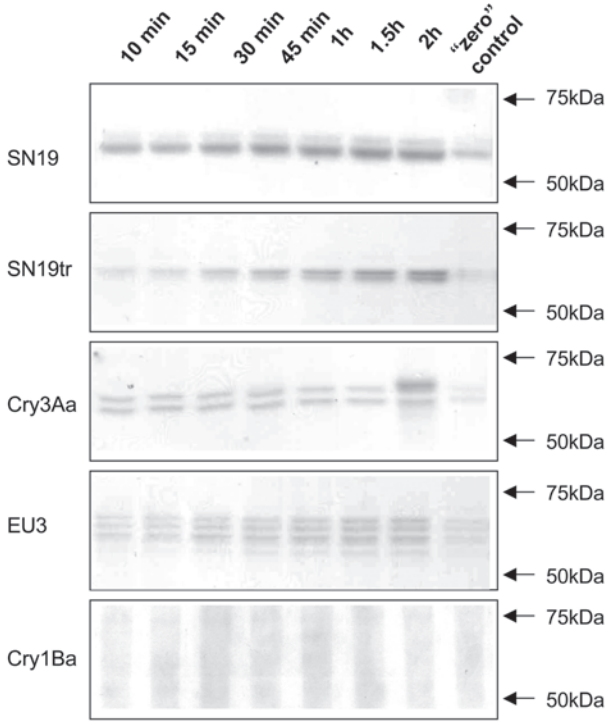

Fig. 6. Time-course experiment of solubilization and proteolytic activation of crystals or inclusion bodies in Colorado potato beetle midgut extract. Crystals or inclusions were incubated for indicated times in diluted CPB gut extracts and soluble proteins from the supernatant were analyzed by SDS-PAGE. Controls contain inclusions and midgut extract prepared for SDS-PAGE immediately after mixing.

SN19 and EU3 seemed to contradict earlier observations with Cry1Ba, in which in vitro solubilization was required for activity against CPB ***(11)***. To understand this phenomenon, we decided to test the ability of CPB gut extract to solubilize and proteolytically activate the four different proteins in crystals or inclusion bodies used in this study. Aliquots of crystals or inclusion bodies were incubated with CPB gut extract at pH 6.5–7.0 and solubilized or activated proteins appearing in the supernatant after fixed times were analyzed by SDS-PAGE. Results of these time-course experiments are shown in **Fig. 6**. Although all crystals and inclusion bodies are stable in water at pH 7.0, all four proteins were retrieved from the supernatant as one or two bands in SDS-PAGE, with the apparent molecular weight of the fully or close to fully activated toxins within the 2 h of the experiment (**Fig. 6**, first four panels). In contrast, when bipyramidal crystals of Cry1Ba were used, no discrete bands corresponding to an activated form were observed (**Fig. 6**, last panel). Thus, the effective solubilization in CPB gut extract of all tested proteins, with the exception of Cry1Ba, correlates well with their activity as crystals or inclusion bodies regardless of whether they have a carboxy-terminal extension, and independent of presolubilization.

4. Discussion

The hybrid proteins used in this investigation—the Cry1 protein SN19 and the Cry3Aa-Cry1Ba hybrid, EU3, both highly active against CPB—

presented an opportunity for a specific study of the contribution of the carboxy-terminal protoxin extension to crystal formation, solubility, and insecticidal activity. In an earlier study, addition of a Cry1Aa carboxy-terminal extension to Cry3Aa decreased the activity of the naturally truncated Cry3Aa and resulted in formation in *B. thuringiensis* of spherical inclusion bodies, from which no full-length fusion protein could be extracted. In *E. coli*, the extended protein formed inclusion bodies and the protein was susceptible to endogenous proteases ***(26)***. In contrast to this, with solubilization the hybrid protein described in this article is at least as active as its truncated form on a per weight basis, which implies that on a molar basis it is more active as the full-length EU3 protein has approximately twice the molecular weight of Cry3Aa. Concurrently, the EU3 protein formed not spherical inclusion bodies but regularly shaped large rectangular or rhomboid crystals in *B. thuringiensis* from which full-length EU3 could be solubilized at high pH, indicating that in this case the addition of a carboxy-terminal extension did not interfere with regular packing of the protein in a crystal, although the crystals were different from those of Cry3Aa. As suggested by the investigators of the earlier study, lack of proper packing in a regular crystal may lead to premature proteolysis of the carboxy-terminal extension by the host cell, in which case only the truncated form of Cry3Aa can be retrieved ***(26)***.

Both SN19, as well as its truncated form SN19tr, formed irregular inclusion bodies in the acrystalliferous *B. thuringiensis* strain. Lack of proper crystal formation of truncated Cry1 proteins has been reported earlier ***(27–30)*** and underlines the function of the carboxy-terminal extension in crystal formation. It was more surprising to find that the full-length SN19, which differs from the bipyramidal crystal-forming Cry1Ba only in its domain II, did not form regular crystals but spherical inclusion bodies. Possibly, disruption of the structure of Cry1Ba protoxin by this replacement interferes with proper packing in the crystals as was found earlier for Cry3Aa protein containing parts substituted by Cry1Ca sequence ***(31)***. Any such perturbation of structure, however, did not very much affect the insecticidal properties of the protein, as SN19 was considerably more active than Cry1Ba against CPB ***(14)***. Despite the lack of regular crystal formation, full-length proteins of the expected molecular weight could be solubilized from the inclusions of SN19 and SN19tr. In vitro solubilization and proteolytic activation of both pairs of CPB active toxins clearly demonstrated that the carboxy-terminal extension did not negatively influence either step in this case. In contrast, no solubilization and proteolytic activation of natural Cry1Ba crystals was observed, which may explain the necessity for solubilization of Cry1Ba to detect activity against CPB ***(11)***.

In conclusion, we have shown that a carboxy-terminal extension does not necessarily preclude activity against CPB, at least for the examples of this study where proteins did not form bipyramidal crystals but irregular inclusions or a rectangular crystal. Whereas earlier reports with Cry1Ba ***(11)*** and Cry7Aa ***(13)*** may already have shown some correlation between bipyramidal crystal formation and lack of activity against CPB, these proteins were not expressed and tested in a truncated form to prove a causal relationship. In contrast, our report shows that lack of proper bipyramidal crystal formation in both EU3 (where it is replaced by another type of crystal formation) as well as in SN19 (where irregular inclusions are formed) is correlated with solubility in CPB gut extract and with CPB activity as crystals or inclusions without the need for presolubilization. This suggests that targeted changes in the crystal-forming ability may be useful in attempts to extend the host range of other *B. thuringiensis* toxins as well.

Acknowledgments

Samir Naimov was supported by a fellowship from the Netherlands Organization for Scientific Research (NWO) International Fellowship Program for Romanian and Bulgarian Postdocs. Elena Uzunova-Martens was supported by an EU-TEMPUS fellowship. We thank Salvador Herrero and Dirk Bosch for critically reading the manuscript.

References

1. de Maagd, R. A., Bravo, A., Berry, C., Crickmore, N., and Schnepf, H. E. (2003) Structure, diversity and evolution of protein toxins from spore-forming entomopathogenic bacteria. *Ann. Rev. Genet.* **37,** 409–433.
2. Vazquez-Padron, R. I., De La Riva, G., Aguero, G., et al. (2004) Cryptic endotoxic nature of *Bacillus thuringiensis* Cry1Ab insecticidal crystal protein. *FEBS Lett.* **570,** 30–36.
3. Bietlot, H., Vishnubhatla, I., Carey, P., Pozsgay, M., and Kaplan, H. (1990) Characterization of the cystein residues and disulphide linkages in the protein crystal of *Bacillus thuringiensis*. *Biochem. J.* **267,** 309–315.
4. Aronson, A. (2002) Sporulation and delta-endotoxin synthesis by *Bacillus thuringiensis*. *Cell. Mol. Life Sci.* **59,** 417–425.
5. Aronson, A. I., Han, E.-S., McGaughey, W., and Johnson, D. (1991) The solubility of inclusion proteins from *Bacillus thuringiensis* is dependent upon protoxin composition and is a factor in toxicity to insects. *Appl. Environ. Microbiol.* **57,** 981–986.
6. Jaquet, F., Hütter, R., and Lüthy, P. (1987) Specificity of *Bacillus thuringiensis* delta-endotoxin. *Appl. Environ. Microbiol.* **53,** 500–504.
7. Schernthaner, J. P., Milne, R. E., and Kaplan, H. (2002) Characterization of a novel insect digestive DNase with a highly alkaline pH optimum. *Insect Biochem. Mol. Biol.* **32,** 255–263.
8. Herrnstadt, C., Soares, G. G., Wilcox, E. R., and Edwards, D. L. (1986) A new strain of *Bacillus thuringiensis* with activity against coleopteran insects. *Bio/Technology* **4,** 305–308.
9. Bernhard, K. (1986) Studies on the delta-endotoxin of *Bacillus thuringiensis* var. *tenebrionis*. *FEMS Microbiol. Lett.* **33,** 261–265.
10. Tailor, R., Tippet, J., Gibb, G., et al. (1992) Identification and characterization of a novel *Bacillus thuringiensis* delta-endotoxin entomocidal to coleopteran and lepidopteran larvae. *Mol. Microbiol.* **6,** 1211–1217.
11. Bradley, D., Harkey, M. A., Kim, M. K., Biever, K. D., and Bauer, L. S. (1995) The insectidal CryIB crystal protein of *Bacillus thuringiensis* ssp. *thuringiensis* has dual specificity to Coleopteran and Lepidopteran larvae. *J. Invertebr. Pathol.* **65,** 162–173.
12. Dow, J. A. T. (1986) Insect midgut function. *Adv. Insect Physiol.* **19,** 187–238.
13. Lambert, B., Höfte, H., Annys, K., Jansens, S., Soetaert, P., and Peferoen, M. (1992) Novel *Bacillus thuringiensis* insecticidal crystal protein with a silent activity against coleopteran larvae. *Appl. Environ. Microbiol.* **58,** 2536–2542.
14. Naimov, S., Weemen-Hendriks, M., Dukiandjiev, S., and de Maagd, R. A. (2001) *Bacillus thuringiensis* delta-endotoxin Cry1 hybrid proteins with increased activity against the Colorado potato beetle. *Appl. Environ. Microbiol.* **67,** 5328–5330.
15. Naimov, S., Dukiandjiev, S., and de Maagd, R. A. (2003) A hybrid *Bacillus thuringiensis* delta-endotoxin gene gives resistance against a coleopteran and a lepidopteran pest in transgenic potato. *Plant Biotechnol. J.* **1,** 51–57.
16. Bosch, D., Schipper, B., van der Kleij, H., de Maagd, R. A., and Stiekema, W. J. (1994) Recombinant *Bacillus thuringiensis* crystal proteins with new properties: possibilities for resistance management. *Bio/Technology* **12,** 915–918.
17. de Maagd, R. A., Weemen-Hendriks, M., Stiekema, W., and Bosch, D. (2000) *Bacillus thuringiensis* delta-endotoxin Cry1C domain III can function as a specificity determinant for *Spodoptera exigua* in different, but not all, Cry1-Cry1C hybrids. *Appl. Environ. Microbiol.* **66,** 1559–1563.
18. de Maagd, R. A., Kwa, M. S. G., van der Klei, H., et al. (1996) Domain III substitution in *Bacillus thuringiensis* delta-endotoxin CryIA(b) results in superior toxicity for *Spodoptera exigua* and altered membrane protein recognition. *Appl. Environ. Microbiol.* **62,** 1537–1543.
19. Herrero, S., Gonzalez Cabrera, J., Ferré, J., Bakker, P. L., and de Maagd, R. A. (2004) Mutations in the *Bacillus thuringiensis* Cry1Ca toxin demonstrate the role of domains II and III in specificity towards *Spodoptera exigua* larvae. *Biochem. J.* **384,** 507–513.
20. Russel, R. M., Robertson, J. L., and Savin, N. E. (1977) POLO: a new computer program for Probit analysis. *ESA Bulletin* **23,** 209–213.
21. Sasaki, J., Asano, S., Iizuka, T., et al. (1996) Insecticidal activity of the protein encoded by the *cryV* gene of *Bacillus thuringiensis* kurstaki INA-02. *Curr. Microbiol.* **32,** 195–200.
22. Yamamoto, T. (1990) Identification of entomocidal toxins of *Bacillus thuringiensis* by high-performance liquid chromatography. *ACS Symp. Ser.* **432,** 46–60.
23. Debro, L., Fitz-James, P., and Aronson, A. (1986) Two different parasporal inclusions are produced by *Bacillus thuringiensis* subsp. *finitimus*. *J. Bacteriol.* **165,** 258–268.
24. McPherson, S., Perlak, F., Fuchs, R., Marrone, P., Lavrik, P., and Fischhoff, D. (1988) Characterization of the coleopteran-specific protein gene of *Bacillus thuringiensis* var. *tenebrionis*. *Bio/Technology* **6,** 61–66.
25. Höfte, H., Seurinck, J., Van Houtven, A., and Vaeck, M. (1987) Nucleotide sequence of a gene encoding an insecticidal protein of *Bacillus thuringiensis* var. *tenebrionis* toxic against Coleoptera. *Nucleic Acids Res* **15,** 7183.
26. Carmona, A. A. and Ibarra, J. E. (1999) Expression and crystallization of a Cry3Aa-Cry1Ac chimerical protein of *Bacillus thuringiensis*. *World J. Microbiol. Biotechnol.* **15,** 455–463.
27. Wabiko, H. and Yasuda, E. (1995) *Bacillus thuringiensis* protoxin-location of toxic border and require-

ment of non-toxic domain for high-level in vivo production of active toxin. *Microbiol* **141,** 629–639.
28. Park, H. W., Bideshi, D. K., and Federici, B. A. (2000) Molecular genetic manipulation of truncated Cry1C protein synthesis in *Bacillus thuringiensis* to improve stability and yield. *Appl. Environ. Microbiol.* **66,** 4449–4455.
29. Adang, M., Staver, M., Rocheleau, T., Leighton, J., Barker, R., and Thompson, D. (1985) Characterized full-length and truncated plasmid clones of the crystal protein of *Bacillus thuringiensis s*ubsp. *kurstaki* HD-73 and their toxicity to *Manduca sexta*. *Gene* **36,** 289–300.
30. Rang, C., Bes, M., Lullienpellerin, V., Wu, D., Federici, B. A., and Frutos, R. (1996) Influence of the 20-kDa protein from *Bacillus thuringiensis* ssp. *israelensis* on the rate of production of truncated Cry1C proteins. *FEMS Microbiol. Lett.* **141,** 261–264.
31. Park, H. W. and Federici, B. A. (2004) Effect of specific mutations in helix alpha7 of domain I on the stability and crystallization of Cry3A in *Bacillus thuringiensis*. *Mol. Biotechnol.* **27,** 89–100.